Quantification of Effects of Global Ischemia on Dynamics of Ventricular Fibrillation in Isolated Rabbit Heart

Ravi Mandapati, MD; Yukio Asano, MD; William T. Baxter, MS; Richard Gray, PhD; Jorge Davidenko, MD; José Jalife, MD

Background—Ventricular fibrillation (VF) leads to global ischemia of the heart. After 1 to 2 minutes of onset, the VF rate decreases and appears more organized. The objectives of this study were to determine the effects of no-flow global ischemia on nonlinear wave dynamics and establish the mechanism of ischemia-induced slowing of the VF rate.

Methods and Results—Activation patterns of VF in the Langendorff-perfused rabbit heart were studied with the use of 2 protocols: (1) 15 minutes of no-flow global ischemia followed by reperfusion (n=7) and (2) decreased excitability induced by perfusion with 5 μmol/L of tetrodotoxin (TTX) followed by washout (n=3). Video imaging ($\approx$7500 pixels per frame; 240 frames per second) with a voltage-sensitive dye, ECG, and signal processing (fast Fourier transform) were used for analysis. The dominant frequency of VF decreased from 13.5±1.3 during control to 9.3±1.4 Hz at 5 minutes of global ischemia ($P<0.02$). The dominant frequency decreased from 13.9±1.1 during control to 7.0±0.3 Hz at 2 minutes of TTX infusion ($P<0.001$). The rotation period of rotors on the epicardial surface (n=27) strongly correlated with the inverse dominant frequency of the corresponding episode of VF ($R^2=0.93$). The core area, measured for 27 transiently appearing rotors, was 5.3±0.7 mm^2 during control. A remarkable increase in core area was observed both during global ischemia (13.6±1.7 mm^2; $P<0.001$) and TTX perfusion (16.8±3.6 mm^2; $P<0.001$). Density of wave fronts decreased during both global ischemia ($P<0.002$) and TTX perfusion ($P<0.002$) compared with control.

Conclusions—This study suggests that rotating spiral waves are most likely the underlying mechanism of VF and contribute to its frequency content. Ischemia-induced decrease in the VF rate results from an increase in the rotation period of spiral waves that occurs secondary to an increase in their core area. Remarkably, similar findings in the TTX protocol suggest that reduced excitability during ischemia is an important underlying mechanism for the changes seen. **(*Circulation*. 1998;98:1688-1696.)**

Key Words: fibrillation ■ ischemia ■ Fourier analysis ■ ventricles ■ excitation

Ventricular fibrillation (VF) has been defined as "turbulent" cardiac electrical activity, which implies a large amount of irregularity in the electrical waves that underlie ventricular excitation. The onset of VF is characterized by very rapid and asynchronous excitation of the ventricles. In the ECG, this is identified by ventricular complexes that are ever changing in frequency, contour, and amplitude. However, it is well known that after 1 to 2 minutes, the rate slows down and the organization of activity appears to increase as VF progresses.[1] Although ischemia-induced reduction in excitability is most likely involved, the precise electrophysiological mechanisms and wave propagation dynamics responsible for these changes during the initial few minutes after the onset of VF remain poorly understood. Paradoxically, VF is more difficult to terminate successfully after >2 minutes of its onset than in the initial stages when activation patterns are more rapid and irregular.[2] Thus it appears to be of obvious clinical benefit to be able to achieve a quantitative understanding of the effects of ischemia on the dynamics of VF so that optimization of defibrillation can be achieved.

Ideally, VF should be explained in terms of electrical waves spreading throughout the 3-dimensional (3-D) myocardium.[3,4] Until recently, limited information was available about the mechanisms responsible for the changes in excitation patterns as global ischemia develops during the course of VF, and most previous reports concentrated on the analysis of the earliest phases of VF or on VF in the total absence of ischemia. For example, Lee et al[5] have shown the presence of reentrant wave fronts with short life spans and meandering cores on the epicardial surface of the ventricles during Wiggers' stage II VF in dogs, which corresponds to the initial 2 minutes after the onset of the arrhythmia. On the other hand, video imaging experiments[6,7] in the well-oxygenated Langendorff-perfused rabbit heart, which permitted the analysis of wave propagation dynamics during long periods of sustained VF under stable experimental conditions, presented direct evidence that VF, as recorded from the epicardium, may result from a small number of spiral waves rotating at high speed along highly complex trajectories. Computer

Received January 6, 1998; revision received May 19, 1998; accepted May 29, 1998.

From the Departments of Pharmacology (Y.A., W.T.B., R.G., J.D., J.J.) and Pediatrics (Cardiology) (R.M.), State University of New York Health Science Center at Syracuse, NY. Dr Gray is presently at Department of Bioengineering, University of Alabama at Birmingham.

Correspondence to Ravi Mandapati, MD, Department of Pharmacology, SUNY Health Science Center at Syracuse, 766 Irving Ave, Syracuse, NY 13210. E-mail mandapar@vax.cs.hscsyr.edu

simulations in a realistic 3-D model of the whole heart[6] suggested that the spiral waves were in fact the 2-dimensional representation of 3-D scroll waves spanning the myocardial wall. In addition, the studies indicated that in the rabbit heart, the degree of organization as viewed by the ECG was well correlated with the extent of movement of a scroll wave. Hence, stationary scroll waves were manifested as monomorphic tachyarrhythmia, whereas the fast-moving scroll waves resulted in ECG patterns that were indistinguishable from VF.[6]

We hypothesize that rotating spiral waves are the most likely underlying mechanism of VF and that ischemia-induced changes in the dynamics of the spiral waves result in changes in the activation patterns during the course of VF. The objectives of this study were 2-fold: first, to determine in the rabbit heart the effects of no-flow global ischemia on nonlinear wave dynamics and to establish the mechanism of ischemia-induced slowing of the VF rate; second, to demonstrate that decreased excitability is one of the mechanisms for the ischemia-induced changes. This was done by creating conditions of decreased excitability through the use of tetrodotoxin (TTX), a sodium channel blocker.[8] Overall, our results demonstrate, for the first time, that decreased excitability leads to increase in the area of the core of rotating spiral waves. These results suggest that increase in core area results in slowing of the VF rate as global ischemia develops during the natural course of VF. Some of these results have been previously presented in abstract form.[9]

Methods

Langendorff-Perfused Rabbit Heart

New Zealand rabbits (weight ≈2 kg) were anesthetized with sodium pentobarbital (60 mg/kg). The chest was opened through a midline incision, and the heart was rapidly removed and connected to a Langendorff apparatus.[10] The coronary arteries were continuously perfused through a cannula in the aortic root with warm (36.5±1°C) HEPES-Tyrode solution under a pressure head of 70 mm Hg. The solution consisted of the following (in mmol/L): HEPES, 15; NaCl, 148; KCl, 5.4; $CaCl_2$, 1.8; $MgCl_2$, 1.0; $NaHCO_3$, 5.8; NaH_2PO_4, 0.4; glucose, 5.5; and albumin, (40 mg/L). The solution (pH 7.4) was saturated with 100% oxygen. The heart was immersed in a rectangular temperature-controlled chamber full of warm HEPES-Tyrode solution that was continuously replenished by the coronary sinus outflow. Care was taken to maintain the epicardial and endocardial temperatures equal and constant at 36.5±1°C. The sinus node was excised, and the AV node was ablated with a portable high-temperature cautery. After this, 2 mL of HEPES-Tyrode solution containing the voltage-sensitive dye di-4-ANEPPS (15 μg/mL) dissolved in DMSO was perfused through the coronaries for 1 to 2 minutes.

ECG Recording

The solution bathing the heart was used as a volume conductor for recording the ECG. Horizontal ECG recordings were obtained with 2 unipolar electrodes immersed in the chamber at equidistant locations from the heart surface.[10] The signals were bandpass-filtered at 0.05 to 1000 Hz (Gould 2400S) and displayed continuously on a digital oscilloscope (Tektronix 2214). Episodes of interest were acquired at a sampling rate of 0.4 ms over 4-second periods, digitized, and transferred to a personal computer (Gateway 2000/P5-60).

High-Resolution Optical Mapping

Details about the experimental setup have been described previously.[11] Briefly, the light from a tungsten-halogen lamp was filtered (520 nm) and then shone on the epicardial surface of the vertically hanging heart. A 50-mm objective lens was used to collect the emitted light, with a depth of field of ≈8 mm. The emitted light was transmitted through an emission filter (645 nm) and projected onto a charge-coupled device video camera (Cohu). The video images (typically 50×150 pixels/or 1500 pixels/cm^2) of the left ventricular epicardial surface, with the left anterior descending coronary artery facing the light source and the camera, were acquired with an A/D frame grabber (Epix) in a noninterlace mode with a speed of 240 frames per second (4.2-ms sampling interval). In the absence of filtering, the spatial resolution was ≈0.15 mm.[11] The frame grabber board was mounted on a Gateway 2000/P5-60 computer that was used to process the imaged data. To reveal the signal, the background fluorescence was subtracted from each frame. Low-pass spatial filtering (weighted average of 15 neighboring pixels) was applied to improve the signals, which resulted in an effective spatial resolution of <0.5 mm (for details see Baxter et al[11]). All the optical recordings were approximately 4 seconds in duration, allowing us to record from 7500 locations simultaneously. During VF, there was minimal motion of the heart. Nevertheless, an adjustable glass wall was used to gently compress and restrain the heart against the fixed wall of the chamber that faced the camera. Such a procedure eliminated motion artifacts almost completely, and thus electromechanical uncoupling agents were not used in these experiments. Optical recordings were obtained during control, ischemia, and reperfusion or during the infusion and washout of 5 μmol/L TTX.

Viability and Integrity of the Heart

At the end of each experiment, the heart was perfused with phosphate-buffered (pH 7.4) tetrazolium chloride for a period of 15 minutes.[12] Any heart that showed evidence of necrosis was excluded from the analysis.

Image and Signal Processing

Isochrone Maps

Isochrone maps were generated from filtered video imaging data, by analyzing the value of each pixel over time. A point in the time plot was labeled as a wave front if it was the fastest part of the upstroke, that is, the maximum first derivative.[11] Thresholds helped to eliminate most maxima caused by noise. Because of motion-induced smearing, a set of pixels perpendicular to the motion of the wave front activated in a single frame. Thus the resulting wave fronts seen in the image data were not lines but bands. Isochrone lines were defined as the borders between wave front bands.

Tracing the Trajectory of Pivoting Points

Short-lasting spiral waves were identified and their rotation periods and core dimensions measured. This was done by tracing the trajectory of the so-called instantaneous pivoting point, a characteristic of spiral waves that does not exist in planar waves or waves initiated by a point source.[13] According to theory, this point is located near the tip of the spiral wave where the front and tail of the rotating wave meet. In a stationary rotating spiral, the trajectory of the pivoting point forms a closed loop that is the perimeter of the core of the spiral wave. The region enclosed by this loop is the area of the core. Figure 1A is a diagram of 2 superimposed consecutive frames (n and n-1) of a spiral wave. The wave front is defined as the newly depolarized area in frame n (upper arrows). The wave tail is defined as the newly repolarized area in frame n (lower arrows). Figure 1B is a diagram of a single frame in which the wave front and wave tail obtained by sequential subtraction of frame n from n-1 along with the pivoting point (p) are shown. At the end of 1 entire cycle, the trajectory of the pivoting point forms the boundary of the core (white circle).

In episodes of VF in which rotating spiral waves were observed, wave fronts and wave tails were determined as follows. The values of gray levels for each site were binarized with a cutoff value of 50% of their maximum value to classify regions as either active (>50%) or repolarized (<50%). After this transformation, the resulting binary images were sequentially subtracted; that is, each frame was

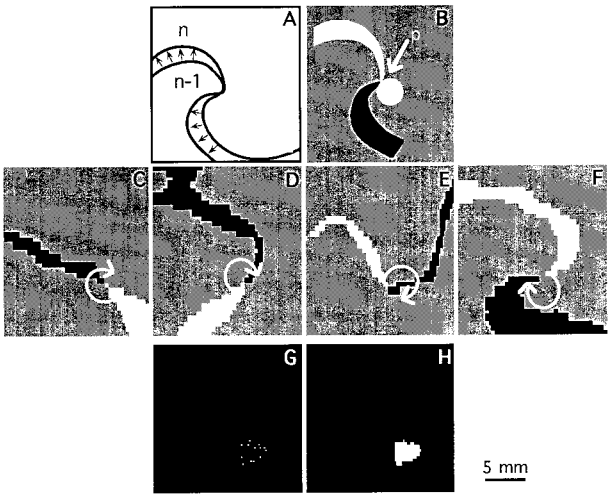

Figure 1. Tracings of the trajectory of pivoting points and measurements of core dimensions. A, Diagram of 2 superimposed consecutive frames (n and n-1) of a spiral wave rotating clockwise. Arrows denote motion of active region defined as area within the isopotential. B, Diagram of a single frame in which wave front and wave tail were obtained by sequential subtraction of frame n from n-1. Also shown are pivoting point (p) and core (white circle). C, D, E, and F show snapshots of wave front and tail at 4.2, 16.7, 29.2, and 41.7 ms, respectively, of a transiently stationary spiral wave rotating clockwise (arrows) at a period of 54 ms. G, Plot of pivoting points of this spiral wave. H, Core of this spiral wave, obtained by connecting consecutive pivoting points.

obtained by subtraction of the previous frame. This resulted in images containing only wave fronts (white) and wave tails (black) that were separated by the pivoting point.

In Figure 1, C, D, E, and F show snapshots at 4.2, 16.7, 29.2, and 41.7 ms, respectively, of a transiently stationary spiral wave having a rotation period of 54 ms. The wave rotated clockwise on the epicardial surface of the left ventricle during an episode of VF in control conditions. The pivoting point was located in every frame for a complete rotation, and its trajectory (13 points for this spiral wave) was plotted as shown in Figure 1G. Consecutive points were connected by straight lines, and the enclosed area (white) is the core of this spiral wave (H).

Quantification of Core Dimensions

The perimeter of the core was defined as the sum of the lengths of the lines connecting the pivot points of 1 complete circuit. The area of the core was calculated from the number of pixels contained within the perimeter of the core.[14]

Quantification of Density of Wave Fronts

The mean number of wave fronts per frame was obtained from the number of wave fronts observed per frame in 50 consecutive frames (200 ms). Density of wave fronts was obtained by dividing the number of wave fronts by the surface area of the entire mapping region.

Electrical Signal Processing

We used a standard signal processing technique, the fast Fourier transform (FFT) to study the spectral content of the ECGs during VF.[15]

Specific Experimental Protocols

The total number of hearts included in the 2 protocols were as follows: (1) global ischemia and VF, 7; (2) TTX and VF, 3.

Effects of Global Ischemia on Activation Patterns of VF

A period of 15 minutes was allowed for stabilization of the Langendorff-perfused heart before the experiment; the ventricles were paced at basic cycle length of 300 ms. Thereafter, the heart was stained, VF was induced by burst pacing at 50 Hz for 2 seconds, and 3 minutes later optical images were obtained from the anterior ventricular epicardial surface. A TTL signal was sent from the stimulator to trigger the oscilloscope so that an ECG was simultaneously recorded. Two to 3 sets of such recordings were obtained during control. No-flow global ischemia was then induced by stopping flow in the aortic cannula and quickly replacing the oxygenated HEPES-Tyrode solution in the chamber with HEPES-Tyrode solution saturated with 100% N_2 and having a pH of 6.8.[16] Optical mapping data and corresponding ECG recordings were obtained at 1, 3, 5, and 10 minutes of ischemia. At this time, reperfusion was started by opening flow in the aortic cannula and replacing the HEPES-Tyrode solution in the chamber with HEPES-Tyrode solution saturated with 100% O_2 at pH 7.4. Epicardial temperature was maintained constant at 36.5±1°C. Optical and ECG data were collected at 1, 3, 5, and 10 minutes of reperfusion.

Effects of TTX on VF

The heart was stabilized, VF was induced, and simultaneous optical and ECG data were obtained during control, as in the global ischemia protocol (see above). The perfusate in the aortic cannula was then switched to HEPES-Tyrode solution containing 5 μmol/L TTX saturated with 100% O_2 and having a pH of 7.4 (TTX dose of 5 μmol/L was selected by titration to consistently obtain stable VF). The solution in the recording chamber remained unchanged. Optical mapping data and corresponding ECG recordings were obtained at 1, 3, and 5 minutes. Washout was then started by switching the perfusate to the original HEPES-Tyrode solution (without TTX), after which optical and ECG data were obtained at 1, 3, and 5 minutes of washout.

Analysis of VF Data

Optical data were spatially filtered for analysis; no temporal filters were applied. Rotating spiral waves were identified by examination of all videos, and the location, rotation period, area, and dimensions of the core of rotating spiral waves were determined by tracing the trajectory of their pivoting points. Density of rotating wave fronts was also measured. Finally, ECGs and their corresponding FFTs were analyzed to examine the changes in ECG patterns and shifts in the dominant frequency. All spiral waves having complete rotations during 10 minutes of control, 5 minutes of ischemia, and 3 and 5 minutes of TTX infusion were included for analyses.

Statistical Analyses

Variables are expressed as mean±SEM. Comparisons were carried out with the use of ANOVA, and significance was determined with the Fisher's protected least-squares test (Statview 4.53, Abacus Concepts). Differences of $P<0.05$ were considered statistically significant. Correlation of the inverse of the dominant frequency with rotation period and core perimeter was performed with the use of simple regression analysis. Slopes are presented with 95% confidence intervals (95% CI). Correlation coefficients (R^2) are presented with associated P values.

Results

Electrocardiographic and Spectral Analysis of VF

The VF patterns recorded by an ECG from the same experiment during control, ischemia, and reperfusion are presented in Figure 2, together with their corresponding frequency spectra. During control (Figure 2), the ECG was highly irregular; yet, not unexpectedly,[17,18] the frequency spectrum was narrow-banded, with a dominant frequency at 14 Hz. In Figure 2, conditions of global ischemia were created. Clearly, after 5 minutes of global ischemia, the heart continued to fibrillate but the VF pattern had become much more regular and the rate was remarkably slower when compared with control. Indeed, as confirmed by the corresponding frequency spectrum, the dominant frequency had decreased to 7.5 Hz. In

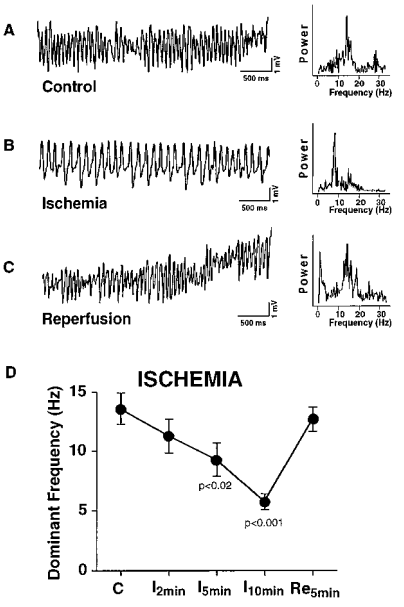

Figure 2. Effects of ischemia on dominant VF frequency. A through C, ECGs and corresponding frequency spectra during VF. A, Control; B, ischemia; C, reperfusion; D, effects of ischemia on dominant VF frequency in 7 experiments. Data from control, 2, 5, and 10 minutes of ischemia, and 5 minutes after reperfusion are shown. *P* values are shown for 5 and 10 minutes of ischemia versus control.

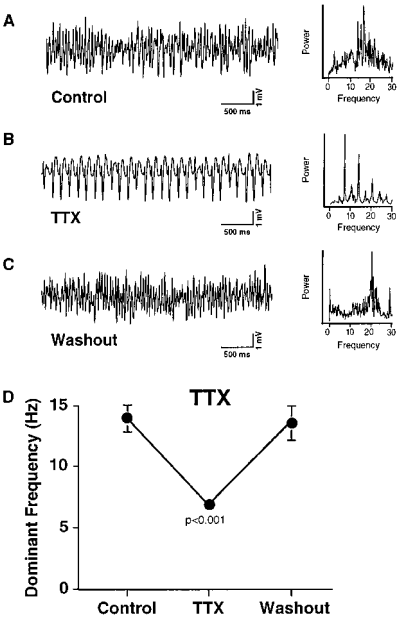

Figure 3. Effects of TTX on dominant VF frequency. A through C, ECGs and corresponding frequency spectra obtained during control (A), TTX perfusion (B), and washout (C). D, Changes in dominant frequency in 3 experiments during control, TTX perfusion, and washout. *P* value is for TTX versus control.

Figure 2, 5 minutes after coronary perfusion was restarted, the irregularity of the arrhythmia had returned to control levels and the dominant peak in the frequency spectrum appeared once again at ≈14 Hz. Similar changes in the dominant frequency of VF were seen in all 7 experiments, as shown in Figure 2. The dominant frequency during control was 13.5±1.3 Hz; it decreased to 11.2±1.4, 9.3±1.4, and 5.7±0.7 Hz, respectively, at 2, 5, and 10 minutes of global ischemia ($P<0.02$, control versus 5 minutes of ischemia), recovering almost back to control levels (12.7±1.0) after reperfusion.

We hypothesized that the dynamics of propagation observed during ischemia were at least partly the result of a significant reduction in excitability. To test this hypothesis, we used the specific sodium channel blocker TTX, based on the idea that the reduced availability of Na channels would reversibly reduce the excitability of the tissue. Figure 3 shows ECGs and their corresponding frequency spectra from episodes of VF induced by burst pacing. Data in Figure 3 were obtained during control; the ECG was highly irregular, yet the frequency spectrum was narrow-banded, with a dominant peak at 17.4 Hz. In Figure 3, conditions of decreased excitability were created by adding 5 μmol/L TTX to the oxygenated HEPES-Tyrode solution. Clearly, after 2 minutes of TTX infusion, VF had become much slower and quite regular, almost resembling ventricular tachycardia. Indeed, as shown by the corresponding frequency spectrum, the dominant frequency had decreased to 6.7 Hz, with several subpeaks denoting harmonics. In Figure 3, after 5 minutes of TTX washout, the irregularity of the arrhythmia had returned to control levels, the spectrum became narrow banded, and the dominant peak increased once again to 21 Hz. Similar changes in the dominant frequency of VF were seen in all 3 experiments, as shown in Figure 3. The dominant frequency during control was 13.9±1.1 Hz and decreased to 7.0±0.3 Hz 2 minutes after starting the TTX perfusion ($P<0.001$, control versus TTX infusion). On washout, the dominant frequency increased to 13.5±1.4 Hz. Overall, these results are remarkably similar to those produced by ischemia and reperfusion (see Figure 2) and support the idea that changes in ventricular excitability may underlie the observed changes in VF frequency and degree of aperiodicity.

Rotating Activity During VF

Our previous video imaging experiments and simulations have demonstrated that in the rabbit heart, VF is characterized by a relatively small number of scroll waves of variable duration.[6,7] Such coexisting scroll waves normally drift and interact with each other in complex ways. In those experiments, the myocardium was constantly being nourished by an oxygenated Tyrode solution, which allowed conditions for "dynamic equilibrium" in the VF patterns. The data presented in A through C of Figure 4 were obtained from a video imaging experiment during a long episode of VF under control conditions. Subsequently, the perfusion was stopped to induce global ischemia. Figure 4A shows a snapshot of the fluorescent image of the preparation as seen by the video camera before background subtraction. The image shows the anterior epicardial ventricular wall with the right ventricle on the left, the left ventricle on the right. The isochrone map in Figure 4B shows 1 full rotation of a drifting spiral wave. The spiral wave became transiently stationary (for 3 rotations) near the apex of the left ventricle, which enabled localization and measurement of the core area (5.2 mm^2; see "Methods"). The wave front rotated in the counterclockwise direction at a

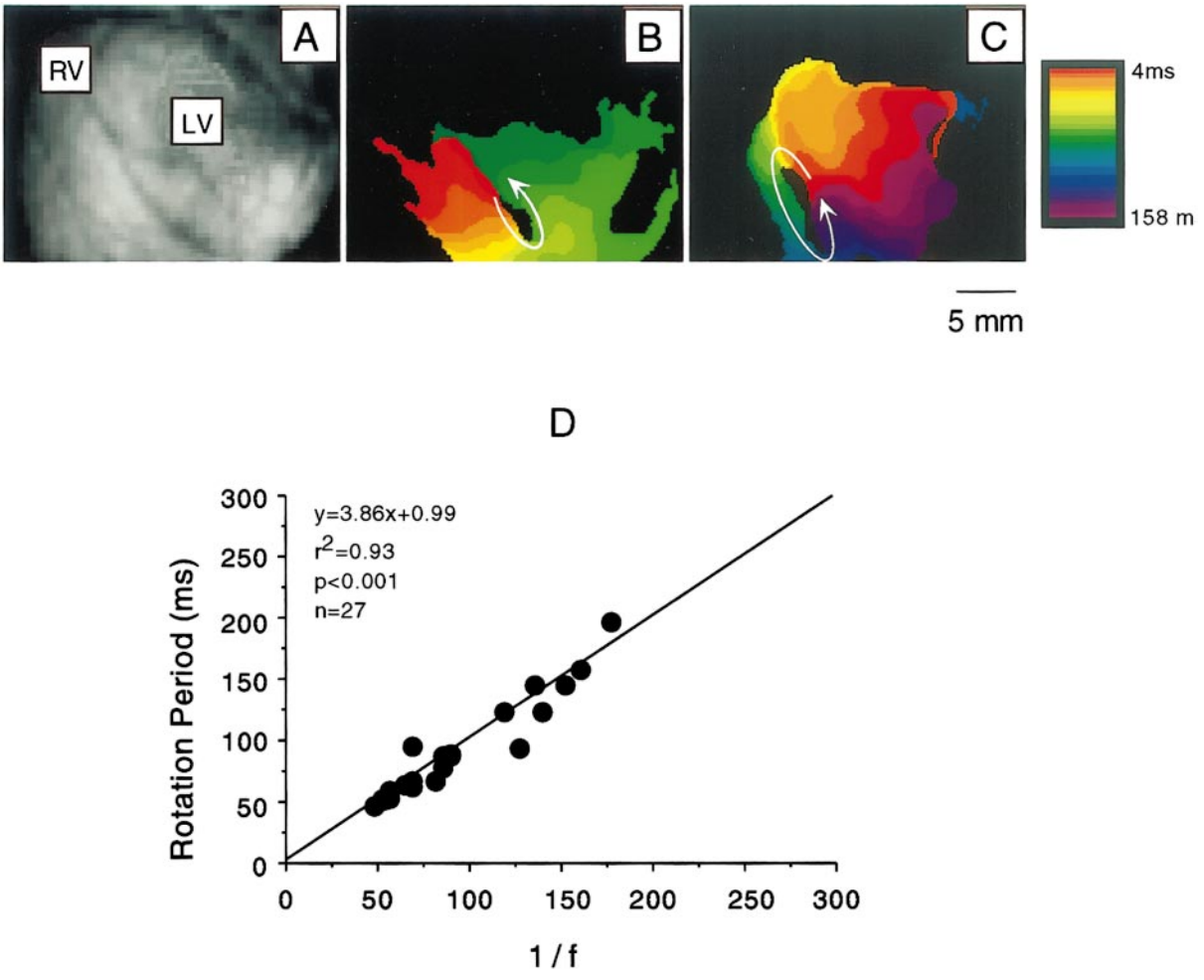

Figure 4. Effects of ischemia on spiral wave dynamics and dominant frequency. Isochrone maps during continuous VF in the same experiment. A, Snapshot of fluorescent image of heart. B, During control, a single wave is shown rotating counterclockwise, with a rotation period of 54 ms. The spiral was stationary for 3 rotations and was subsequently replaced by different dynamics (not shown). C, At 5 minutes of ischemia, a different spiral wave is shown rotating counterclockwise with a rotation period of 158 ms. Color bar where each color band corresponds to 4.2 ms of activity, with red representing earliest activation and purple representing latest activation, is shown adjacent to C. D, Correlation between rotation period of 27 individual rotors and inverse dominant frequency (1/f) from the power spectrum of their corresponding episodes of VF. RV, Right ventricle; LV, left ventricle.

period of 54 ms. The effect of global ischemia (5 minutes) on the same episode of VF is shown in Figure 4C. The isochrone map obtained during ischemia also shows a counterclockwise, rotating spiral wave that appeared transiently near the apex of the left ventricle. However, under these conditions, the core was much larger (area=14.4 mm^2) and the rotation period was remarkably slower (158 ms) than in control.

Rotation Period Correlates With Dominant Frequency in FFT

On the basis of previous evidence favoring the idea that rotating spiral waves are the underlying mechanism of VF,[6,7] we hypothesized that the rotation period of such spirals determines the dominant frequency in the ECG. Rotation periods of 27 different rotors during VF in the global ischemia and TTX experiments were correlated with the inverse dominant frequency (1/f) in the power spectrum of the corresponding episode of VF. As shown in Figure 4D, the strong correlation (R^2=0.93, slope=0.99, and 95% CI 0.88 to 1.1) between these 2 parameters suggests that the periodicity of rotating spiral waves is the main contributor to the dominant frequency in the ECG during VF. In addition, the high correlation between the rotation period of individual rotors and the global activity recorded by the ECG suggests that under a given condition, multiple spiral waves will have a narrow range of rotation periods. Such uniformity of rotation periods is attended by uniformity in the size of the core of spiral waves (see below).

Core Dimensions Determine Dominant Frequency of VF

Analysis of VF dynamics during control and ischemia in the data shown in Figure 4 suggested that ischemia-induced prolongation in the cycle length of the individual spiral waves and the accompanying shift in the dominant peak in the VF spectrum were closely associated with an increase of the path of the spiraling wave front around its center of rotation (compare core areas in B and C of Figure 4). Core dimensions of rotating spiral waves were determined by tracing the trajectory of their pivoting points (see "Methods"). In Figure

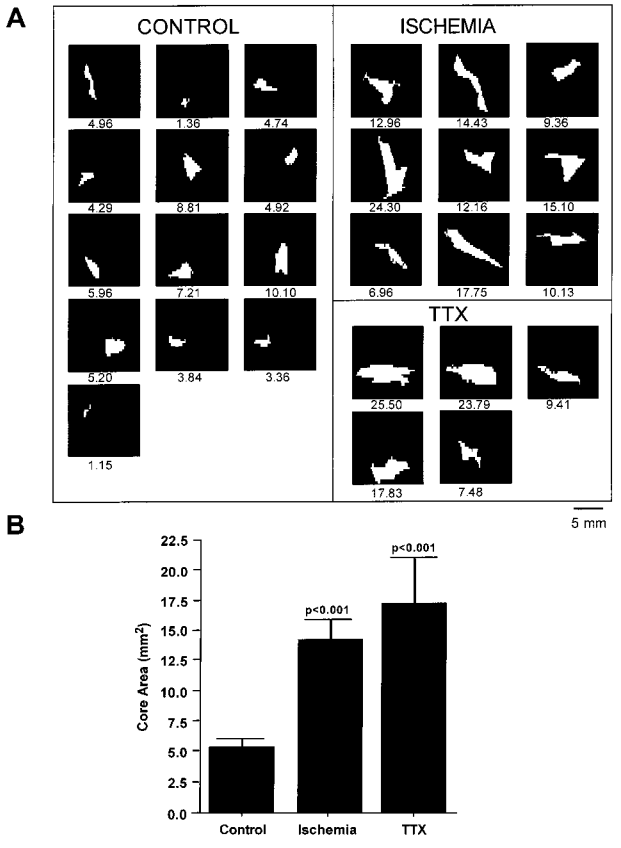

Figure 5. Measurements of core area. A, Left: Cores of 13 individual spirals recorded during control. A, Right: 9 representative cores seen during 5 to 10 minutes of global ischemia; on the bottom are 5 cores seen during TTX infusion. In all cases, numbers under each frame indicate core area in mm^2. Quantitative comparisons of core areas in the 3 conditions are shown in B. *P* values are for ischemia versus control and TTX versus control.

5A, cores of spiral waves during control (n=13), global ischemia (n=9), and TTX (n=5) perfusion are shown in white. In all cases, somewhat elongated but asymmetrical cores were inscribed. During control conditions, the cores were relatively small. When the fibrillating heart was exposed to conditions of decreased excitability induced by either global ischemia or TTX perfusion, the measured cores were much larger.

Quantification of the area of the core is presented in Figure 5B. Significant increases in core area were seen during both global ischemia and TTX infusion. In control, the core had a mean area of 5.1±0.7 mm^2. The core area increased dramatically during global ischemia to 13.6±1.7 mm^2 ($P<0.001$). A similar increase to 16.8±3.6 mm^2 was also observed during TTX infusion ($P<0.001$). To provide definite proof that the observed increase in rotation period of spiral waves underlying VF is secondary to an increase in the perimeter of the core (ie, the path traveled by the pivoting point to complete a single rotation), we correlated the rotation periods of the 27 rotors (cores shown in Figure 5) with their respective core perimeters. As shown in Figure 6, an increase in the perimeter of the core results in an increase in the rotation period ($R=0.82$; $P<0.001$). The relatively low R^2 value (0.67) may indicate contamination by other factors, including decrease in

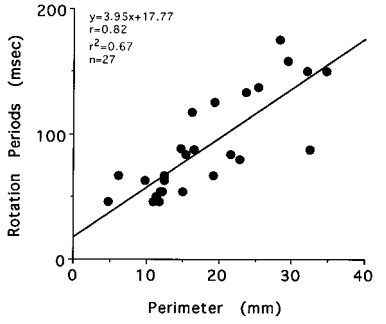

Figure 6. Correlation between the rotation period of 27 individual waves and perimeter of their cores.

the conduction velocity at the pivoting point of the rotating wave front. Nevertheless, the results strongly suggest that the slowing of VF frequency during ischemia results from an increase in the core area.

Changes in Density of Rotors During VF

From the foregoing, it is clear that changes in the size of the core around which short-lived spirals rotate are the most important determinant of the effects of ischemia and of TTX infusion on VF frequency. Since in either case the core area increases as much as 3 times from control (see Figure 5D), one would expect that the number of coexisting rotors (ie, their density) at a given instant during VF should be lower during global ischemia or TTX infusion than in control. In addition, ischemia-induced increase in refractoriness should also cause a decrease in the density of wave fronts. To test this conjecture, we measured the density of wave fronts (see "Methods") during control and after induction of global ischemia or perfusion with TTX. As shown in Figure 7A, the density of wave fronts during control was 1.23±0.18/cm^2 and decreased to 0.93±0.14/cm^2 and 0.55±0.03/cm^2 at 2 and 5 minutes of ischemia, respectively ($P<0.002$ control versus 5 minutes ischemia). Reperfusion resulted in reversal of the

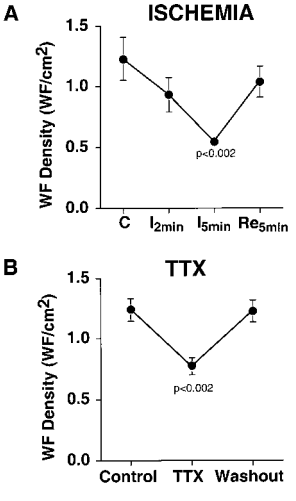

Figure 7. Effects of ischemia on density of VF wave fronts (WF) measured on epicardium (see "Methods" for further details). A, Density of rotating wave fronts during control, ischemia, and reperfusion. B, Density of rotating wave fronts during control, TTX infusion, and washout. *P* values are for 5 minutes ischemia versus control and for TTX versus control.

changes with an increase in the density of wave fronts to near control ($1.04\pm0.13/cm^2$). A similar change was also observed during perfusion of TTX, as shown in Figure 7B. The density of wave fronts during control was $1.24\pm0.09/cm^2$ and decreased to $0.77\pm0.07/cm^2$ at 2 minutes of TTX perfusion ($P=0.002$, control versus TTX). Washout of TTX resulted in an increase in the density of wave fronts to $1.22\pm0.09/cm^2$.

Discussion

This study provides the first quantification of the changes in the activation patterns of VF induced by global ischemia, which most probably has an important influence on the natural course of the arrhythmia. Using high resolution optical mapping, we have demonstrated that rotating spiral waves are most likely the underlying mechanism of VF and contribute to its frequency content. Most importantly, we have established for the first time that the mechanism of ischemia-induced decrease in the VF rate is an increase in the area of the cores around which such waves rotate. Perfusion of the preparation with a sodium channel blocker (TTX) resulted in remarkably similar findings, indicating that reduced excitability during ischemia is an important mechanism for the changes seen.

Dynamics of Rotors and VF

Recently, application of the nonlinear dynamics theory to the study of wave propagation in the heart,[19,20] together with high-resolution mapping techniques,[13] has enabled investigators to think of VF as a problem of self-organization of nonlinear electrical waves with both deterministic and stochastic components. This has led to the application of new experimental and numerical approaches to the study of the 2-dimensional and 3-D spatio-temporal patterns of excitation that result in VF.[6,7] Overall, the data presented in those studies strongly support the hypothesis that VF in the structurally normal heart is not a totally random phenomenon. VF may be explained in terms of self-organized 3-D electrical rotors giving rise to scroll waves that drift throughout the heart at varying speeds.[6] For example, a recent study has revealed that in the rabbit heart, even a single rotor that drifts rapidly throughout the ventricles can give rise to complex patterns of cardiac muscle excitation.[6] In the ECG, such patterns cannot be distinguished from VF. On the other hand, a rotor that anchors to a discontinuity or defect in the cardiac muscle (eg, a scar, a large artery, or a bundle of connective tissue) is expected to result in stationary rotating activity.[19] The latter is manifested in the ECG as so-called "monomorphic" ventricular tachycardia. In the case of VF, data suggest that it is usually the result of a relatively small number of coexisting but short-lived rotors. The rotors may drift and interact with each other and with boundaries in the heart, resulting in annihilation and/or formation of new but also short-lived rotors. The end result would be complex spatio-temporal patterns of excitation throughout the ventricles. Overall, the demonstration of drifting spiral waves in cardiac muscle has paved the way for a better understanding of the mechanisms of the changes in VF dynamics induced by global ischemia or by sodium channel blockade.

Evolution of Global Ischemia–Induced Electrophysiological Changes

The classic cinematographic and electrocardiographic studies in the in situ canine heart done by Wiggers[1] in 1930 provided the first demonstration that after its onset, uninterrupted VF goes through 4 successive stages.[1] During the first 2 stages (which together last 1 to 2 minutes), activation is quite rapid, with a cycle length of 90 to 120 ms, and the activation rate then progressively slows in the last 2 stages. Slowing is most likely caused by ischemia because it is prevented by perfusing the coronary arteries during fibrillation, as observed during control in our experiments and also previously demonstrated in the canine heart.[21] The progressive ionic and metabolic changes that are observed in the ventricular myocardium during the course of ischemia have been well described.[22–24] Moreover, it is likely that as a result of reduced excitability,[25] ischemia-induced changes in the critical curvature for propagation of rotating wave fronts plays an important role in modifying the patterns of activation during the course of VF.

Effect of Changes in Core Dimensions on VF

Our analyses demonstrate that the dominant frequency of VF decreases from ≈13 Hz in the control to ≈9 Hz after 5 minutes of global ischemia (Figure 2). Simultaneously, there was a highly significant increase in the core area from ≈5 mm^2 during control to ≈14 mm^2 at 5 minutes of global ischemia (see Figure 5B). Similarly, the rotation period increased primarily consequent to an increase in the perimeter of the spiral tip trajectory (see Figure 6), as demonstrated by the regression analysis between the rotation period and the perimeter of their cores ($r=0.82$). These data suggest that during global ischemia, the pivoting point of the spiral wave travels a longer distance to complete a rotation leading to an increase in the rotation period, which in turn results in slowing of the VF rate. Additionally, decreased conduction velocity during ischemia may also result in an increase in the rotation period of spiral waves. The final product of our analysis is the demonstration that rotating spiral waves are the main contributors to the frequency content of VF, as shown by the strong correlation ($R^2=0.93$) between the rotation period of such waves and inverse dominant frequency (1/f) in the power spectrum of the corresponding episode of VF. This result also suggests that under a given condition, multiple spiral waves in the same heart will have a narrow range of rotation periods.

Effects of TTX on VF Dynamics

The effect of TTX on the ECG pattern, VF rate, core area, and rotation period were remarkably similar to those observed during global ischemia, indicating that the changes seen in the activation patterns of VF during its natural course (modified by global ischemia) are primarily the result of a decrease in excitability. These experiments also suggest that among the many ionic mechanisms underlying the changes seen in VF during global ischemia, decreased sodium conductance probably plays a significant role.

Wave Front Curvature and Increase in Core Size

The results presented here may be explained on the basis of the theory of wave propagation in excitable media, which considers wave front curvature a major determinant of conduction velocity. The theory predicts that there is a critical radius of curvature at which propagation ceases.[26] This is especially true in the case of spiral waves because the wave front has a very pronounced curvature close to the tip. If, in a given excitable medium, the critical radius of curvature is very small, then the tip of the spiral wave may undergo sharp turns, leading to a small core area. On the other hand, if the critical radius of curvature is relatively large, then the tip of the spiral wave will follow a more linear trajectory, which in turn will lead to an increase in the area of the core. Thereby the perimeter of the core, which corresponds to the trajectory of the pivoting tip of the wave front, is determined by the critical radius of curvature in that medium. Experimental and numerical studies in isolated cardiac muscle (Cabo et al[25]) and other excitable media (Krinsky et al[27]) have shown that changes in excitability are followed by changes in the critical radius of curvature such that the lower the excitability, the larger is the critical radius of curvature. Under conditions of nominal excitability, the critical radius of curvature is small, which, in the case of reentry, manifests as a rapidly rotating spiral around a small core. However, under conditions of decreased excitability (eg, during global ischemia or TTX perfusion) the critical curvature becomes large, and, consequently, the trajectory of the pivoting point also increases; thereby the path taken by the wave front to complete a full rotation is longer, resulting in an increase in the size of the core and a prolongation of the rotation period.

Limitations of the Study

The high spatial resolution and large field of view of the video camera provide an invaluable tool for the study of cardiac arrhythmias in the isolated heart. However, our study has some limitations that must be considered and may be summarized as follows: (1) Video imaging of potentiometric dye fluorescence in these experiments confines the analysis to the epicardial activation patterns during VF; it does not give any information about activity within the ventricular wall. However, as demonstrated by previous numerical and experimental studies from our laboratory,[6,7] the only mechanism that explains the patterns of electrical activity that we recorded on the epicardial surface (spiral waves) during VF in the isolated rabbit heart is nonstationary 3-D scroll waves. (2) Although TTX is a convenient tool to study the effects of reduced excitability on wave propagation patterns, it does not reproduce the effects of ischemia. Particularly, TTX is not known to reduce resting membrane potential, which is one of the major effects of ischemia.[23] Nevertheless, the changes observed on VF dynamics during TTX perfusion were strikingly similar to those resulting from ischemia, which gives us confidence that excitability is indeed an important parameter to be concerned with in these experiments. (3) The image obtained by the charge-coupled device camera is not a direct measure of voltage but of fluorescence; therefore there is no true transmembrane potential reference for the optical signal. (4) Bleaching may be a significant problem. The cumulative oxidation of dye molecules on light absorption reduces the fluorescence of the dye during the course of an experiment and has been a limiting factor with many potentiometric dyes. The long bleaching time of di-4-ANEPPS makes it a useful probe for many trials of long recording. Moreover, restaining of the heart allows the reestablishment of the fluorescence to the initial levels, and this may be done several times in the course of a long experiment. (5) During VF, contraction is uncoordinated and quite weak; occasionally there was a need to restrain the heart to reduce the mechanical artifact. We placed the heart between 2 glass plates and applied moderate levels of pressure on the plates that reduced the motion adequately. To the above list of limitations we must add those that are specific to the video camera system; that is, relatively low signal-to-noise ratio, which occasionally requires spatial filtering, resulting in a reduction of the effective spatial resolution of the system, and relatively low temporal resolution (4.2 ms per frame), which prohibits the detailed analysis of very high-frequency phenomena, such as determining the upstroke velocity of the action potential. The latter, however, was not an impediment for accurate quantitative measurement of slow-moving spiral wave dynamics. Future developments of video optical mapping will most likely focus on faster and more sensitive video cameras as well as voltage-sensitive dyes with greater signal-to-noise ratio.

Despite the above limitations, the study provides robust quantitative information about VF dynamics in control as well as during ischemia and reperfusion. The results enhance our understanding of such dynamics and give insight into mechanisms causing the changes in activation patterns during the natural course of VF. It is hoped that such new knowledge could be the basis for improved strategies for defibrillation.

Acknowledgments

This study was supported in part by grant PO1-HL39707 from the National Heart, Lung, and Blood Institute, National Institute of Health. Dr Yukio Asano was supported by grant 960183 from the American Heart Association, New York State Affiliate. We would like to thank Jiang Jiang, Jiangping Chen, Megan Flanagan, Tatiyana Yuzyuk, and Laverne Gilbert for their technical assistance.

References

1. Wiggers C. Cinematographic and electrocardiographic observations of the natural process in the dog's heart: its inhibition by potassium and the revival of coordinated beats by calcium. *Am Heart J*. 1930;5:351–365.
2. Yakaitis RW, Ewy A, Otto CW, Taren DL, Moon TE. Influence of time and therapy on ventricular defibrillation in dogs. *Crit Care Med*. 1980; 8:157–163.
3. Chen PS, Wolf PD, Dixon EG, Daniely ND, Frazier DW, Smith WM, Ideker RE. Mechanism of ventricular vulnerability to single premature stimuli in open chest dogs. *Circ Res*. 1988;62:1191–1209.
4. Pertsov AM, Jalife J. Three dimensional vortex-like reentry. In: Zipes DP, Jalife J, eds. *Cardiac Electrophysiology: From Cell to Bedside*, 2nd ed. Philadelphia, Pa: WB Saunders Co; 1995:403–410.
5. Lee JJ, Kamjoo K, Hough D, Hwang C, Fan W, Fishbein MC, Bonometti C, Ikeda T, Karagueuzian H, Chen PS. Reentrant wave fronts in Wiggers' stage II ventricular fibrillation. *Circ Res*. 1996;78:660–675.
6. Gray RA, Jalife J, Panfilov A, Baxter WT, Cabo C, Davidenko JM, Pertsov AM. Mechanisms of cardiac fibrillation. *Science*. 1995;270: 1222–1225.
7. Gray RA, Pertsov A, Jalife J. Spatial and temporal organization during cardiac fibrillation. *Nature*. 1998;392:75–78.
8. Sakakibara Y, Wasserstrom A, Furukawa T, Jia H, Arenzen CE, Hartz RS, Singer DH. Characteristics of the sodium current in single human atrial myocytes. *Circ Res*. 1992;71:535–546.

9. Mandapati R, Asano Y, Davidenko JM, Gray RA, Baxter WT, Jalife J. Effects of global ischemia on propagation during ventricular fibrillation in the isolated rabbit heart. *J Am Coll Cardiol*. 1997;330A:29. Abstract.
10. Gray RA, Jalife J, Panfilov A, Baxter WT, Cabo C, Davidenko JM, Pertsov AM. Nonstationary vortexlike reentrant activity as a mechanism of polymorphic ventricular tachycardia in the isolated rabbit heart. *Circulation*. 1995;91:2454–2469.
11. Baxter WT, Davidenko JM, Loew, LM, Wuskell JP, Jalife J. Technical features of a CCD camera system to record cardiac fluorescence data. *Ann Biomed Eng*. 1997;25:713–725.
12. Nassif G, Dillon SM, Rayhill S, Wit AL. Reentrant circuits and the effects of heptanol in a rabbit model of infarction with a uniform epicardial border zone. *J Cardiovasc Electrophysiol*. 1993;4:112–133.
13. Davidenko JM, Pertsov AV, Salomonsz R, Baxter W, Jalife J. Stationary and drifting spiral waves of excitation in isolated cardiac muscle. *Nature*. 1992;355:349–351.
14. Jähne B. *Practical Handbook on Image Processing for Scientific Applications*. Boca Raton, Fla: CRC Press; 1997.
15. Press WH, Teukolsky SA, Vetterling WT, Flannery BP. *Numerical Recipes in C*. 2nd ed. New York, NY: Cambridge University Press; 1992.
16. Yan GX, Kleber AG. Changes in extracellular and intracellular pH in ischemic rabbit papillary muscle. *Circ Res*. 1992;71:460–470.
17. Goldberger AL, Bhargava V, West BJ, Mandell AJ. Some observations on the question: Is ventricular fibrillation "chaos"? *Physica D*. 1986;19:282–289.
18. Herbshleb JN, Heethaar RM, van der Tweel I, Meijler FL. Frequency analysis of the ECG before and during ventricular fibrillation. *Computers in Cardiology*. Long Beach, Calif: IEEE Computer Society; 1981:365–368.
19. Pertsov AV, Davidenko JM, Salomonsz R, Baxter W, Jalife J. Spiral waves of excitation underlie reentrant activity in isolated cardiac muscle. *Circ Res*. 1993;72:631–650.
20. Winfree AT. *When Time Breaks Down*. Princeton, NJ: Princeton University Press; 1987.
21. Worley SJ, Swain JL, Colavita PG, Smith WM, Ideker RE. Development of an endocardial-epicardial gradient of activation rate during electrically induced sustained ventricular fibrillation in the dog. *Am J Cardiol*. 1985;55:813–820.
22. Kleber AG, Fleischhauer J, Cascio WE. Ischemia induced propagation failure in the heart. In: DP Zipes, J Jalife, eds. *Cardiac Electrophysiology: From Cell to Bedside*. Philadelphia, Pa: WB Saunders Co; 1995:174–182.
23. Cascio WE, Johnson TA, Gettes LS. Electrophysiologic changes in the ischemic ventricular myocardium, I: Influence of ionic, metabolic and energetic changes. *J Cardiovasc Electrophysiol*. 1995;6:1039–1062.
24. Gettes LS, Buchanan JW Jr, Saito T, Kagiyama Y, Oshita S, Fujino T. Studies concerned with slow conduction. In: Zipes DP, Jalife J, eds. *Cardiac Electrophysiology and Arrhythmias*. Orlando, Fla: Grune & Stratton, Inc; 1985:81–87.
25. Cabo C, Pertsov AM, Baxter WT, Davidenko JM, Gray RA, Jalife J. Wave front curvature as a cause of slow conduction and block in isolated cardiac muscle. *Circ Res*. 1994;75:1014–1028.
26. Zykov VS. *Simulation of Wave Processes in Excitable Media*. New York, NY: Manchester University Press; 1987.
27. Krinsky VI, Efimov IR, Jalife J. Vortices with linear cores in excitable media. *Proc R Soc Lond*. 1992;437:645–655.

Quantification of Effects of Global Ischemia on Dynamics of Ventricular Fibrillation in Isolated Rabbit Heart

Ravi Mandapati, Yukio Asano, William T. Baxter, Richard Gray, Jorge Davidenko and José Jalife

Circulation. 1998;98:1688-1696
doi: 10.1161/01.CIR.98.16.1688
Circulation is published by the American Heart Association, 7272 Greenville Avenue, Dallas, TX 75231

Print ISSN: 0009-7322. Online ISSN: 1524-4539